Available online at www.sciencedirect.com
ScienceDirect
Polymer 48 (2007) 2939–2945
polymer
www.elsevier.com/locate/polymer

Novel PVA–silica nanocomposite membrane for pervaporative dehydration of ethylene glycol aqueous solution

Ruili Guo, Xiaocong Ma, Changlai Hu, Zhongyi Jiang*

Key Laboratory for Green Chemical Technology, School of Chemical Engineering and Technology, Tianjin University, No. 92, Weijin Road, Nakai District, Tianjin 300072, China

Received 12 December 2006; received in revised form 7 February 2007; accepted 12 March 2007
Available online 16 March 2007

Abstract

To effectively suppress the swelling of poly(vinyl alcohol) (PVA) membrane, polymer–inorganic nanocomposite membranes composed of PVA and γ-mercaptopropyltrimethoxysilane (MPTMS) were prepared by in situ sol–gel technique for pervaporative separation of water–ethylene glycol (EG) mixtures. Effects of the types of catalyst for sol–gel process and MPTMS content on the physical and chemical structure of PVA–silica nanocomposite membranes (designated as PVA–MPTMS hereafter) were investigated by ^{29}Si NMR, FTIR, SEM, XRD and TGA–DTA. Due to the formation of more compact crosslinked structure, nanocomposite membranes exhibited enhanced thermal stability. It was found that when 50 wt% of MPTMS was incorporated into PVA, the nanocomposite membranes possessed optimum pervaporation performance for 80 wt% EG aqueous solution at 70 °C. Unexpectedly, there was no improvement in the pervaporation performance of PVA–MPTMS nanocomposite membranes after mercapto group was oxidized into sulfonic group.

Keywords: Poly(vinyl alcohol)–silica; Nanocomposite membranes; Pervaporation dehydration

1. Introduction

Polymer–inorganic nanocomposite materials are promising systems for many applications due to their extraordinary properties arising from the synergism between the properties of these two different building blocks [1,2]. Some studies have revealed that introducing inorganic component derived from Si-containing precursor into an organic polymer can form a homogeneous nanocomposite membrane with enhanced physicochemical stability and separation performance [3–9]. In our previous study, we have prepared PVA–silica nanocomposite membranes by the in situ sol–gel reaction of γ-glycidyloxypropyltrimethoxysilane (GPTMS) and tetraethoxysilane (TEOS) within poly(vinyl alcohol), the formed silica particles and crosslinking network between silica particle and PVA effectively suppressed the swelling of PVA and exhibited desirable stability in EG aqueous solution, as well as high diffusion selectivity for water [10]. However, the increased hydrophobicity due to the depletion of hydrophilic hydroxyl groups, led to these nanocomposite membranes exhibiting lower sorption selectivity for water. Hence, in order to obtain high selectivity and permeability for water, sufficient amount of polar groups should be present in the hybrid membrane matrix. It is well known that silane-coupling agents ($(R')_n$–Si–$(OR)_{4-n}$) are usually utilized directly as inorganic precursors for sol–gel process [9,11,12]. During sol–gel process, alkoxy groups (R) hydrolyze in the presence of water, and then form the crosslinking network between the formed inorganic silica particles and organic polymer through condensation reactions. In addition, the organic group R′ containing hydrophilic and hydrophobic functional groups, such as $-NH_3$, , H_2C=CH–, –SH group etc., endows the nanocomposite membrane with different properties. In this work, we choose mercapto group containing precursor 3-mercaptopropyltrimethoxysilane

* Corresponding author. Tel./fax: +86 022 27892143.
E-mail address: zhyjiang@tju.edu.cn (Z. Jiang).

0032-3861/$ - see front matter © 2007 Elsevier Ltd. All rights reserved.
doi:10.1016/j.polymer.2007.03.035

(MPTMS) as silica source due to the following considerations: the inherent hydrophilicity of −SH group, the facile conversion of −SH group into more hydrophilic sulfonic acid group [13–16].

In this study, silica particles were incorporated into PVA matrix to prepare PVA–silica nanocomposite membrane by in situ sol–gel reaction of MPTMS within PVA. The effects of sol–gel catalyst type and MPTMS content on the structure of PVA–MPTMS nanocomposite membranes and pervaporation performance for EG aqueous solution were investigated.

2. Experimental sections

2.1. Materials and membrane preparation

Poly(vinyl alcohol) (PVA) (the degree of polymerization and saponification were 1750 ± 50 and 99%, respectively), ethylene glycol, hydrochloric acid, aqueous ammonia and hydrogen peroxide were purchased from Tianjin Guangfu Fine Chemical Research Institute (Tianjin, China). γ-Mercaptopropyltrimethoxysilane (MPTMS) was purchased from Beijing Shenda Fine Chemical Co. Ltd. (Beijing, China). All the chemicals were of analytical grade and used without further purification. Double distilled water was used throughout the study.

PVA was dissolved in double distilled water at 90 °C for 1 h to obtain 7 wt% PVA homogeneous solution. The hot solution was filtered, a certain amount of MPTMS and 1 M HCl or NH_4OH were then added into the filtrate and the mixture was stirred for 12 h at room temperature. The PVA solutions with different MPTMS contents were cast onto an organic glass plate with the aid of a casting knife, dried at room temperature for 2–3 days, and then the completely dried membranes were subsequently peeled off and annealed at 80 °C for 2 h, then at 150 °C for 8 h. The average thickness of membranes was 45 ± 5 μm, measured by micrometer. The resulting PVA control membrane and PVA–silica nanocomposite membranes were designated as PVA and PVA–MPTMS*x*, where *x* was 10, 25, 50 and 67 wt%, which indicated the weight percentage of MPTMS in the initial PVA/MPTMS composition.

Oxidation treatment of PVA–MPTMS nanocomposite membranes: the annealed PVA–MPTMS nanocomposite membranes were oxidized by 5 wt% hydrogen peroxide in an acetone solution at 40 °C for 10 h. Then, the resulting membranes were thoroughly washed with double distilled water.

2.2. Membrane characterization

FTIR spectra were recorded on a Nicolet, 5DX instrument equipped with both horizontal attenuated total reflectance (HATR) accessories. Thirty-two scans were accumulated with a resolution of 4 cm^{-1} for each spectrum. Solid-state NMR spectra were recorded on an Infinity Plus-300 MHz spectrometer. Solid samples were spun at 3 kHz. The morphology of nanocomposite membranes was examined by Philips XL-30 M scanning electron microscope (SEM) instrument. Structures of PVA and PVA–MPTMS nanocomposite membranes were studied using PAN Analytical X-ray diffractometer in the range of 5–50° at the speed of 8°/min (Co Kα 40 kV/200 mA). The degradation process and the thermal stability of the samples were investigated using thermogravimetric analysis (TGA) (Perkin–Elmer TG/DTA thermogravimetric). TGA was conducted under a continuous flow of nitrogen using a heating rate of 10 °C/min from 50 to 800 °C. X-ray photoelectron spectra (XPS) were acquired with a PHI-1600 (PE USA) spectrometer equipped with an Mg Kα ($h\nu = 1486.6$ eV) as radiation source. Survey spectra were collected over a range of 0–1100 eV and high-resolution spectra of C 1s, O 1s, Si 1s and S 2p were also collected. The take-off angle of the photoelectron was set at 90°. Contact angles were measured at 20 °C by using contact angle goniometer (JC2000C, Powereach Co., Shanghai, China). Each measurement was repeated three times and then averaged for the final results. The errors were within ±5%.

2.3. Pervaporation experiments

Pervaporation experiments were performed on the membrane module (CM-Celfa AG Company, Switzerland). The effective membrane area was 25.6 cm^2. The vacuum in the downstream side was maintained (6 Torr) using a vacuum pump. The permeate was collected in liquid nitrogen-cold traps. The compositions of the feed and permeate were measured using Agilent 6890 gas chromatography equipped with a TCD detector and a column packed with GDX102 (Tianjin Chemical Reagent Co., China). The pervaporation performance of the nanocomposite membranes is evaluated by two parameters, flux J, which is defined as $J = Q/A\Delta t$, and separation factor α, which is defined as $\alpha = (y_W/y_{EG})/(x_W/x_{EG})$, where Q is the mass of permeate sample collected in time Δt, A is the effective membrane area, and x and y represent the weight fractions of water (W) and ethylene glycol (EG) in the feed and permeate, respectively.

3. Results and discussion

3.1. Characterization of nanocomposite membranes

3.1.1. The effect of acidic and basic catalysts on the morphological structure of PVA–MPTMS nanocomposite membranes

The structure of mercaptopropyl–silica in PVA matrix that resulted from hydrolysis and condensation of MPTMS using acidic or basic catalyst can be clearly analyzed through ^{29}Si solid-state NMR experiments. The ^{29}Si NMR chemical shift of MPTMS approximately appears at −48 ppm (T_1, RSi(OSi)$(OX)_2$, (X = H or CH_3)), −58 ppm (T_2, RSi$(OSi)_2(OX)$), and −68 ppm (T_3, RSi$(OSi)_3$) [17]. It can be seen from Fig. 1 that there exist two peaks T_2 and T_3 based on the condensation mechanism of MPTMS. The area under the T_2 and T_3 peaks is proportional to the population of linear and cyclic methylpolysiloxane structures, respectively. Therefore, the ratio of peak intensity of T_3 to T_2 (T_3:T_2) can reflect the relative strength

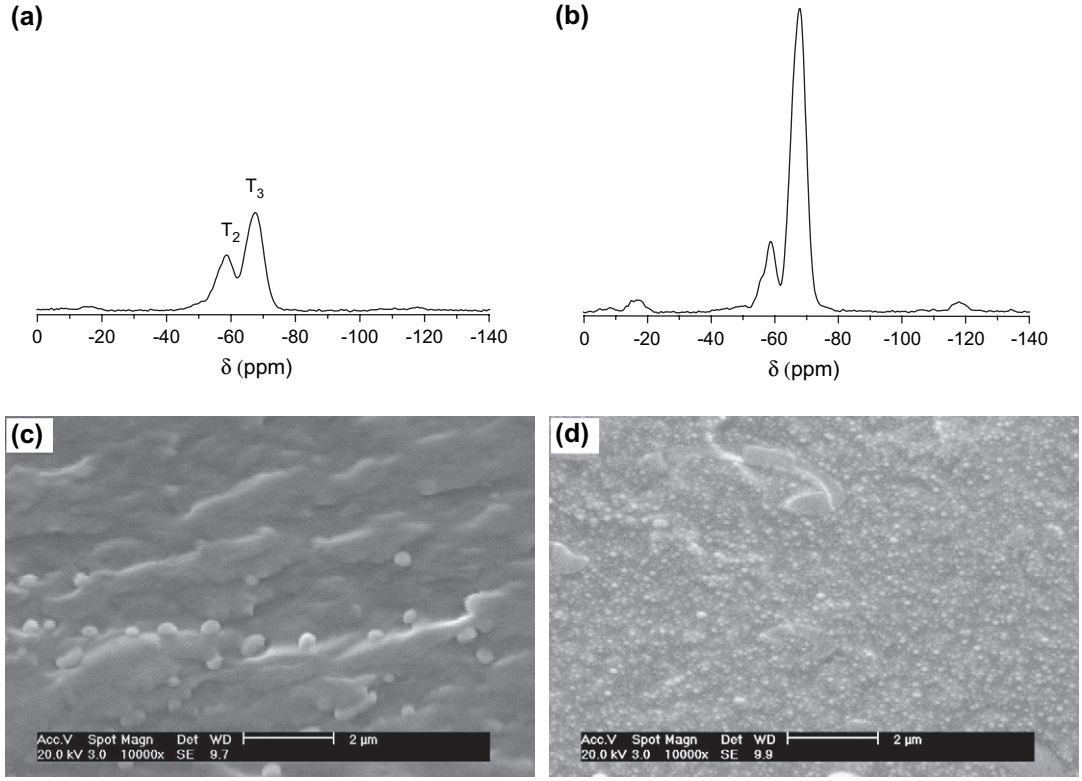

Fig. 1. ^{29}Si NMR spectra and SEM cross-section of PVA–MPTMS50 nanocomposite membrane prepared using acidic (a, c) and basic (b, d) catalysts.

of cyclic silica structure in PVA–MPTMS nanocomposite membranes. Obviously, the relative ratio of peak intensity to signal in basic media (5.56) is much larger than that in acidic media (1.92). Generally, differences in hydrolysis rate will influence the relative number of monomers having one, two or three silanol groups. In turn, these relative abundances will affect the condensation rate and the ultimate degree of condensation achieved. Hence, it can be deduced that the hydrolysis of alkoxylsilanes of MPTMS is much more complete under basic condition, which strengthens the crosslinking between PVA and silica by dehydration and dealcoholysis reactions, while more hydrolyzates exist in the form of T_2 type under acidic condition, which usually does not form inorganic silica particles but rather a linear, weakly crosslinked nanocomposite structure [18–20]. In addition, the morphology can be seen from the cross-section images of SEM in Fig. 1c and d. Under basic media, spherical silica nanoparticles were homogeneously distributed within PVA matrix, while under acidic media, linear and lightly branched silica particles were unevenly distributed. The different structures and distributions of silica particles in the nanocomposite membranes will correspondingly lead to different pervaporation performances.

3.1.2. Effect of MPTMS content on the structure of PVA–MPTMS nanocomposite membranes

It is well known that the reinforcing capacity of inorganic particles in nanocomposite membranes depends on the content of the inorganic particles in the polymer matrix. Consequently, the effects of MPTMS content on the chemical and physical structure of PVA–MPTMS nanocomposite membranes in the basic media are investigated herein.

Fig. 2 shows the FTIR spectra of PVA membrane and PVA–MPTMS nanocomposite membranes in the range of 4000–2500 cm^{-1} and 1700–750 cm^{-1}. The absorption peak at 1000–1100 cm^{-1} is assigned to the stretching vibration of C–O and C–O–C groups in PVA. An increase in the absorbance of the peak at 1000–1100 cm^{-1} of PVA–MPTMS

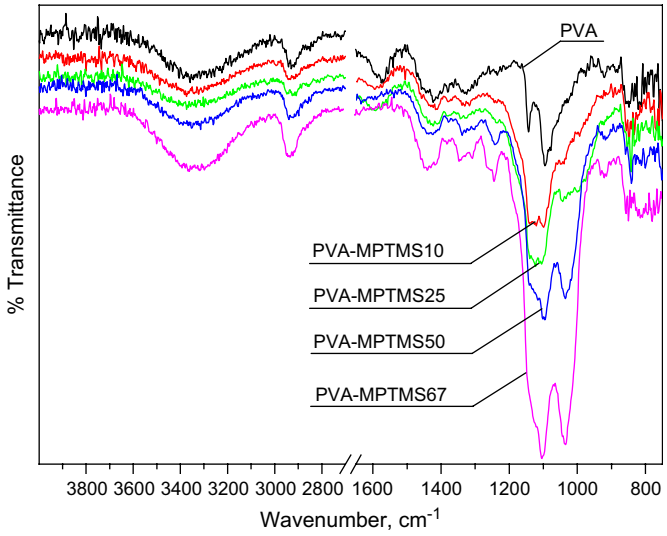

Fig. 2. FTIR spectra of control PVA membrane and PVA–MPTMS nanocomposite membranes prepared under basic condition.

nanocomposite membranes is attributed to the formation of Si–O–C (1045 cm^{-1}) and Si–O–Si (1095 cm^{-1}) bonds [21]. The Si–O–Si group is the result of condensation reaction between hydrolyzed silanol Si–OH groups and the Si–O–C groups may be originated from the condensation reaction between Si–OH groups from hydrolyzed MPTMS and C–OH groups from PVA. Hence, the presence of Si–O–C and Si–O–Si bonds confirmed the existence of covalent linkage between the organic groups and the silica, which led to better compatibility and crosslinking network between organic and inorganic components.

The morphology of nanocomposite membranes with different MPTMS content was studied by SEM images and is presented in Fig. 3. It can be observed that when MPTMS content is 50 wt%, the homogeneous distribution of silica particles at a nanoscale level (average size: 200 nm) is achieved in PVA matrix. However, when MPTMS content is more than 50 wt%, the silica particles tend to aggregate, and inhomogeneous, bigger silica particles appear in PVA matrix. In addition, the effect of formed silica particles on the crystallinity of PVA was investigated by WAXD with a Co Kα source and is shown in Fig. 4. The control PVA membrane and the nanocomposite membranes exhibit a typical peak at 23.0°, which shows its semi-crystalline nature. However, the nanocomposite membrane peaks show lower strength compared to that of control PVA membrane. Furthermore, the peak intensity decreases with increasing MPTMS content. These results imply that the interaction between the silica particles and PVA substantially destroys the formation of crystalline regions.

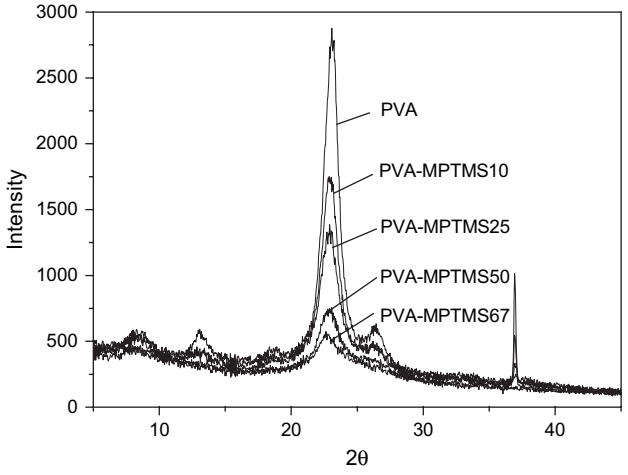

Fig. 4. X-ray diffraction patterns of control PVA membrane and PVA–MPTMS nanocomposite membranes prepared under basic condition.

3.1.3. Thermal stability of PVA–MPTMS nanocomposite membranes with different MPTMS content

The thermal stability of PVA–MPTMS nanocomposite membranes was investigated by TGA–DTA measurements and is shown in Fig. 5a and b. Two main degradation steps can be clearly observed from the DTG curves (Fig. 5b). The first decomposition temperatures of pure PVA, due to the elimination of side-groups at lower temperature, occurred at 200–325 °C, followed by a less evident one between 400 and 500 °C corresponding to the decomposition of main chain of PVA. Comparatively, the first decomposition temperatures

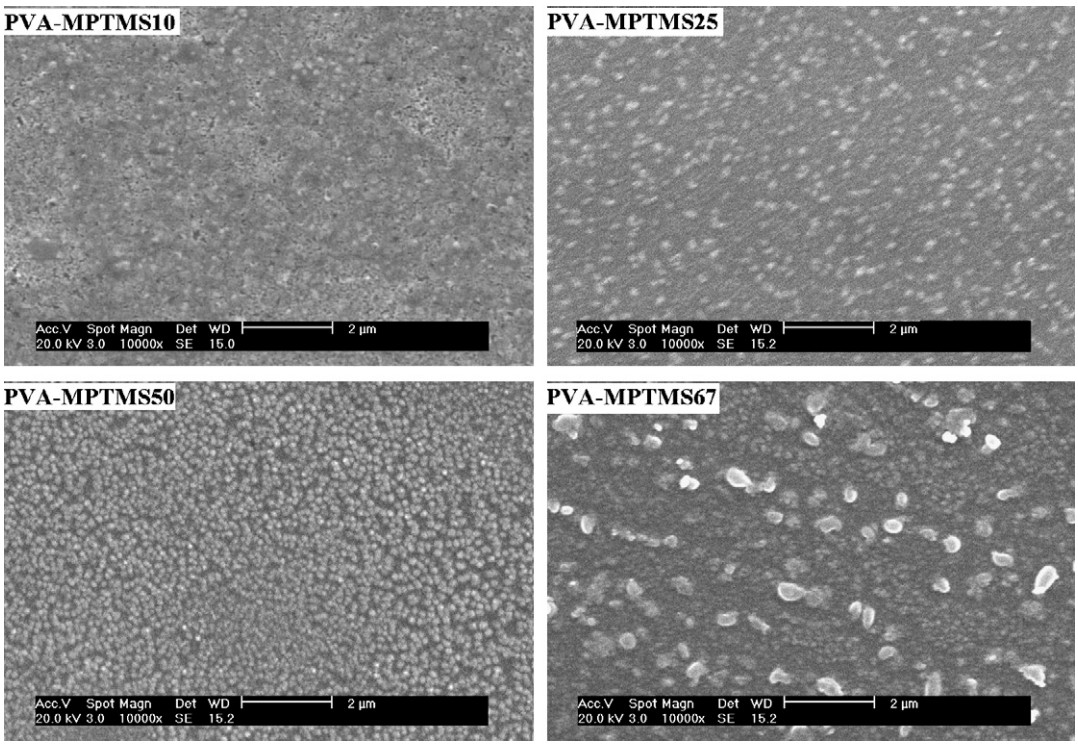

Fig. 3. SEM surface images of PVA–MPTMS nanocomposite membranes prepared under basic condition.

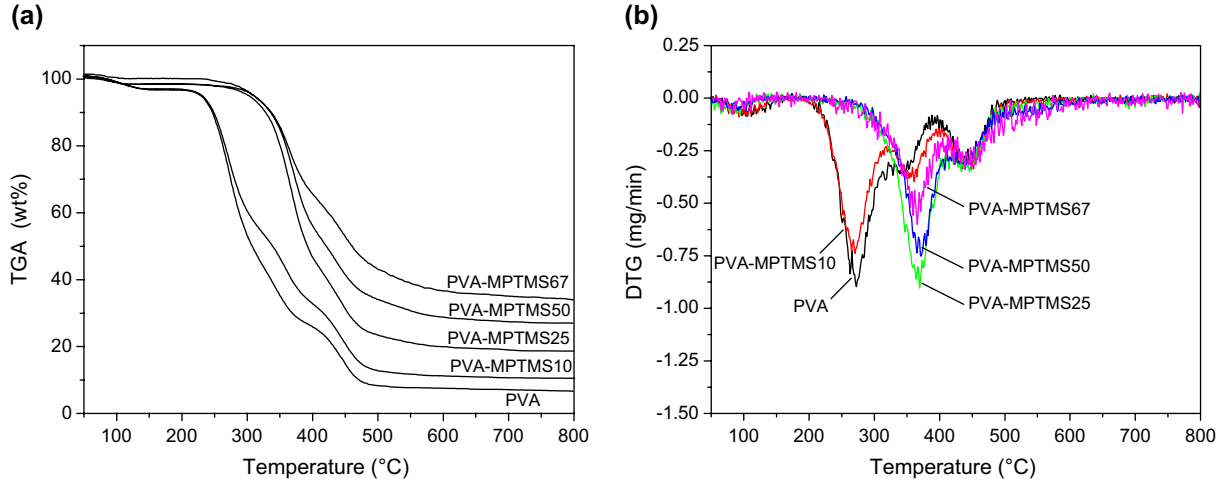

Fig. 5. TGA (a) and DTA (b) measurements of control PVA membrane and PVA–MPTMS nanocomposite membranes prepared under basic condition.

and residual weight of PVA–MPTMS nanocomposite membranes (Fig. 5a) become higher than those of control PVA membrane with increasing MPTMS content. These results suggest that the introduction of silica into the PVA chains enhances the thermal stability of the given nanocomposite materials, which may be attributed to the high thermal stability of silica and the nature of crosslinking network between the silica phase and PVA bulk [22].

3.2. Pervaporative performance of PVA–MPTMS nanocomposite membranes

3.2.1. The pervaporation performance of PVA–MPTMS50 nanocomposite membrane prepared using basic and acidic catalysts

PVA–MPTMS nanocomposite membranes prepared using acidic and basic catalysts possess different structural characteristics and exhibit different pervaporation performances. As to water–EG (80 wt% EG) mixtures at 70 °C and 100 L/h feed flow rate, permeation flux and separation factor of PVA–MPTMS50 nanocomposite membrane prepared under basic condition are 67 g m^{-2} h^{-1} and 311, respectively, while the corresponding values of PVA–MPTMS50 nanocomposite membrane prepared under acidic condition are 84 g m^{-2} h^{-1} and 44. The reason is that in an acidic catalyst system, hydrolysis of the alkoxylsilanes is not complete and the subsequent condensation reaction leads to weak crosslinking of PVA–MPTMS nanocomposite membrane. However, in a basic catalyst system, the well-dispersed silica nanoparticles and the well-established three-dimensional crosslinking network effectively inhibit the swelling of PVA in EG aqueous solution and enhance the separation factor for water. It should be mentioned here that the membranes used in the following sections are all PVA–MPTMS nanocomposite membranes prepared under basic conditions.

3.2.2. The effect of MPTMS content on pervaporation performance of PVA–MPTMS nanocomposite membranes

The changes of the MPTMS content in nanocomposite membranes with respect to their permeation flux and separation factor for EG aqueous solution during pervaporation are illustrated in Fig. 6. These results suggest that PVA–MPTMS nanocomposite membranes are water selective. It is noticed that the permeation flux decreases with increasing MPTMS content up to 50 wt% in the matrix, and then increases when MPTMS content increases beyond 50 wt%. The change of separation factor is just reverse, and shows a maximum value at MPTMS content of 50 wt%. The reason is that when 50 wt% MPTMS is introduced into PVA bulk, the given size of silica particles and homogeneous distribution make the silica particles maximize the possible attachment points with the polymer, that is, the crosslinking density of the silica particles and PVA chains can be effectively increased. Hence, higher separation factor and lower permeation flux are obtained. However, when the MPTMS content increases up to 67 wt%, the silica particle tends to form aggregates, which weakens the crosslinking between the PVA and silica particles. This change leads to the decrease of separation factor and the increase of permeation flux of the nanocomposite membrane.

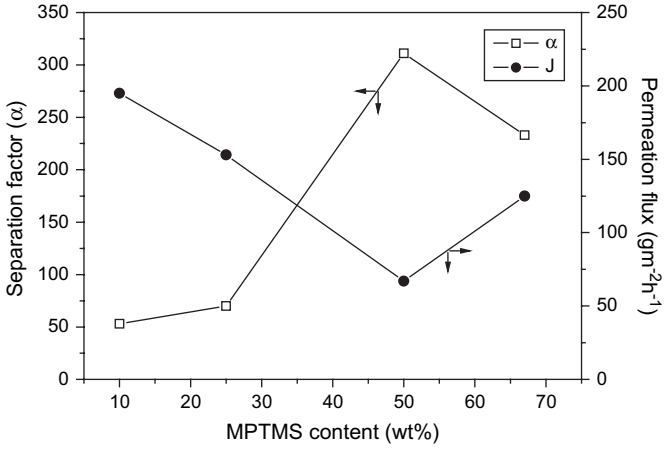

Fig. 6. Effect of MPTMS content on the pervaporation performance of PVA–MPTMS nanocomposite membranes prepared under basic condition for 80 wt% EG aqueous solution in the feed at 70 °C.

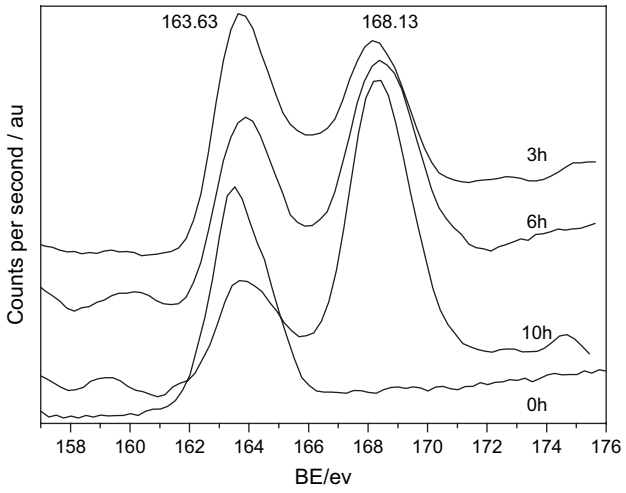

Fig. 7. XPS spectra in the S 2p core level region of PVA–MPTMS50 nanocomposite membranes (prepared under basic condition) oxidized at 40 °C for different times.

3.2.3. The effect of oxidation on pervaporation performance of PVA–MPTMS nanocomposite membranes

To enhance the hydrophilicity of the nanocomposite membranes, oxidation of −SH into the corresponding sulfonic group was conducted in acetone solution contains 5 wt% H_2O_2 at 40 °C for different times. XPS measurement was used to evaluate the oxidation degree of mercapto groups to sulfonic groups. Fig. 7 shows two types of sulfur species: one at lower BE (163.63 eV), corresponding to an −SH group, and the other at higher BE (168.13 eV), associated with sulfonic $-SO_3H$ group [23]. The ratio of intensity at 168.13 eV to 163.63 eV is employed to evaluate the oxidation degree of mercapto group to $-SO_3H$ group. The oxidation degree of mercapto group increases with increase of oxidation time as shown in Table 1. But substantially lower sulfur contents than unoxidized sample are found from the continuous decrease of the ratio of Si to S. This decrease suggests that long-term oxidation leads to substantial loss of S element from the surface of nanocomposite membrane, which may

Table 1
Atomic percent and binding energy (eV) of S 2p level of PVA–MPTMS50 nanocomposite membranes oxidized in 5 wt% H_2O_2 at 40 °C for different times

Oxidation time (h)	C at%	O at%	Si at%	S at%	Si/S	S 2p	
						163 eV (%)	168 eV (%)
0	67.7	18.7	8.5	4.8	1.77	100.0	0
3	71.1	18.7	6.6	2.3	2.87	54.1	45.9
6	69.3	21	5.9	2.0	2.85	41.3	58.7
10	70.4	21.7	5.3	1.6	3.31	19.8	78.2

Table 2
Contact angle of control PVA membrane, unoxidized and oxidized PVA–MPTMS nanocomposite membranes prepared under basic conditions (20 °C)

Contact angle (°)	PVA	PVA–MPTMS10	PVA–MPTMS25	PVA–MPTMS50	PVA–MPTMS67
Without oxidation	58.58	49.80	48.44	46.91	43.43
Oxidation	–	46.91	44.48	43.27	41.17

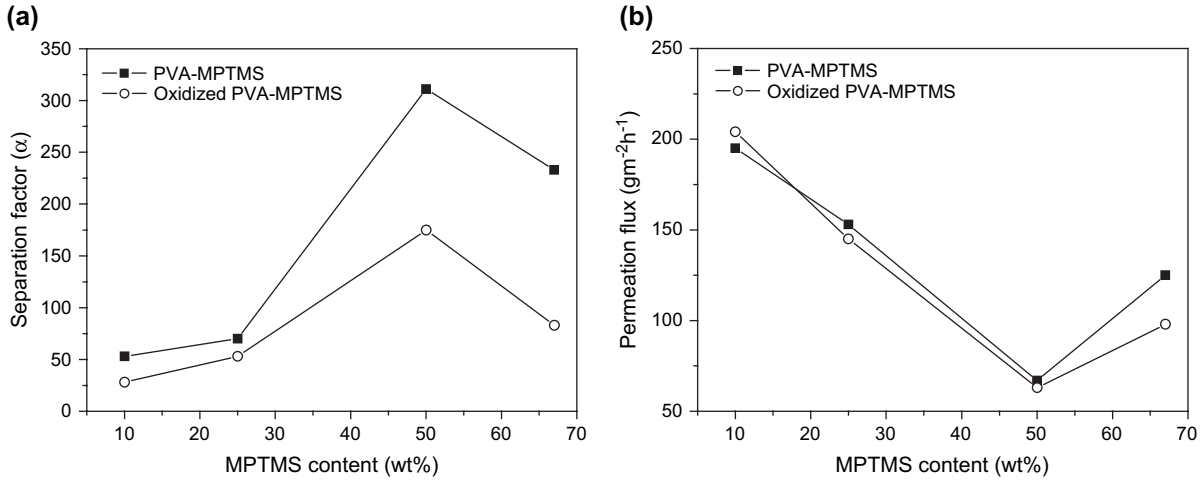

Fig. 8. The comparison of pervaporation performance between the unoxidized PVA–MPTMS nanocomposite membranes and oxidized PVA–MPTMS nanocomposite membranes prepared under basic condition.

be due to the lower thermal stability of sulfonic groups [24]. In order to confirm whether the hydrophilicity of nanocomposite membrane is enhanced by −SH oxidation method, the static contact angles for methylene iodide on the surfaces of PVA–MPTMS and oxidized PVA–MPTMS (oxidized for 10 h) nanocomposite membranes were measured as shown in Table 2. It can be clearly seen that the hydrophilicity of unoxidized nanocomposite membrane is significantly lower than that of control PVA membrane while all the oxidized PVA–MPTMS nanocomposite membranes become more hydrophobic.

The pervaporation performance of oxidized PVA–MPTMS nanocomposite membranes for dehydration from 80 wt% EG aqueous solution is observed from Fig. 8. The separation factor of all oxidized nanocomposite membranes is less than that of unoxidized membranes (Fig. 8a), and little change on the permeation flux is also found (Fig. 8b). The reason is that an increase of hydrophobicity reduces the membrane selectivity for water and increases the permeation of EG through the membranes.

4. Conclusions

PVA–silica nanocomposite membranes were prepared under acid- and base-catalyzed sol–gel reaction of MPTMS within PVA matrix. It was found that spherical, nanoscale silica particles were generated and homogeneously distributed in PVA matrix under basic condition. The covalent bond and hydrogen bond between the silica particles and PVA chains increased their compatibility and crosslinking. In addition, the incorporation of silica particles into PVA caused desirable changes in the morphology and crystalline structure of the films, and significantly enhanced the thermal stability and stability of the membranes in EG aqueous solution. When 50 wt% MPTMS was introduced into PVA bulk under basic conditions, the resulting nanocomposite membrane showed desirable separation factor of 311 with a permeation flux of 67 $g\,m^{-2}\,h^{-1}$ for dehydration from 80 wt% EG aqueous solution at 70 °C. However, there was no improvement in the pervaporation performance of PVA–MPTMS nanocomposite membranes after mercapto group was oxidized into sulfonic group.

Acknowledgements

The authors are grateful for the financial support from the Cross-Century Talent Raising Program of Ministry of Education of China and the Program for Changjiang Scholars and Innovative Research Team in University from the Ministry of Education of China, and Petrochina Research Program (No. W050509-02-02).

References

[1] Ulbricht M. Polymer 2006;47(7):2217–62.
[2] Khayet M, Villaluenga JPG, Valentin JL, López-Manchado MA, Mengual JI, Seoane B. Polymer 2005;46(23):9881–91.
[3] Yan L, Li YS, Xiang CB. Polymer 2005;46(18):7701–6.
[4] Uragami T, Okazaki K, Matsugi H, Miyata T. Macromolecules 2002;35(24):9156–63.
[5] Uragami T, Matsugi H, Miyata T. Macromolecules 2005;38(20):8440–6.
[6] Liu YL, Su YH, Lee KR, Lai JY. J Membr Sci 2005;251:233–8.
[7] Gomes D, Nunes SP, Peinemann K-V. J Membr Sci 2005;246:13–5.
[8] Ohshima T, Matsumoto M, Miyata T. Macromol Chem Phys 2005;206(4):473–83.
[9] Peng FB, Lu LY, Sun HL, Wang YQ, Liu JQ, Jiang Z. Chem Mater 2005;17(26):6790–6.
[10] Guo RL, Hu CL, Pan FS, Wu H, Jiang Z. J Membr Sci 2006;281:454–62.
[11] Wu FC, Chen T-Y, Wan C-C, Wang Y-Y, Lin T-L. Electrochem Solid-State Lett 2006;9(12):A549–51.
[12] Liu YL, Su YH, Lai JY. Polymer 2004;45(20):6831–7.
[13] Shang XY, Li XH, Xiao M, Meng YZ. Polymer 2006;47(11):3807–13.
[14] Munakata H, Chiba H, Kanamura K. Solid State Ionics 2005;176:2445–50.
[15] Margolese D, Melero TA, Christiansen SC, Chmelak BF, Sturcky GD. Chem Mater 2000;12(8):2448–59.
[16] Nagarale RK, Gohil GS, Shahi VK, Rangarajan R. Macromolecules 2004;37(26):10023–30.
[17] Innocenzi P, Brusatin G, Babonneau F. Chem Mater 2000;12(12):3726–32.
[18] Zera TW, Artaki I, Jonas J. J Non-Cryst Solids 1986;80:365–79.
[19] Mauritz KA, Warren RM. Macromolecules 1989;22(4):1730–4.
[20] Robertson MAF, Mauritz KA. J Polym Sci Part B Polym Phys 1998;36:595–606.
[21] Innocenzi P. J Non-Cryst Solids 2003;316:309–19.
[22] Holland BJ, Hay JN. Polymer 2001;42(16):6775–83.
[23] Cano-Serrano E, Blanco-Broeva G, Campos-Martin JM, Fierro JLG. Langmuir 2003;19(18):7621–7.
[24] Evans PJ, Slade RCT, Varcoe JR, Young KE. J Mater Chem 1999;9(12):3015–21.